LYCEN 9601
February 1996

Direct observation of multi-ionization and multi-fragmentation in high velocity cluster-atom collision.

B. Farizon, M. Farizon, M. J. Gaillard, E. Gerlic, R. Genre, S. Louc,
Institut de Physique Nucléaire de Lyon, IN2P3 - CNRS et Université Claude Bernard
43, Boulevard du 11 Novembre 1918, 69622 Villeurbanne Cedex, France.
and
N. V. de Castro Faria, G. Jalbert
Instituto de Fisica, Universidade Federal do Rio de Janeiro
Cx. p. 68528, Rio de Janeiro, RJ, 21945-970, Brazil

Abstract

We report on a direct observation of multi-ionization of the H_{21}^{+} hydrogen cluster in a single collision with a helium atom at 60 keV/u. Up to quadruple ionization of the cluster was observed and new multi-fragmentation channels were detected. Besides that, the results show two different fragmentation processes of doubly charged clusters H_{21}^{2+} : emission of a dimer H_2^{+}, or emission of a trimer H_3^{+} after a rearrangement in the cluster prior to fragmentation.

PACS : 36.40.+d
Keywords : high-energy cluster collision, fragmentation phenomena, cluster multi-fragmentation, multi-ionization process, Coulombic explosion, ionic hydrogen clusters

To be published in Chemical Physics Letters

1. Introduction

Atomic cluster physics has been developed extensively in several directions for van der Waals clusters [1] and for metallic clusters [2]. Recently, the availability of high-energy cluster beams has opened a large field for new experiments, especially cluster fragmentation studies involving high-energy cluster-atom collisions. Fragmentation phenomena have been observed in many different areas of physics [3,4]. A fragmentation process following a collision or some other method of excitation produces a distribution of constituents of the system. Examples are, e.g., meteoritic distributions reaching the earth, avalanche and sandpile slides, lunar crater sizes, droplet sizes in aerosols, nucleus and atomic cluster fragmentation, etc. Under some initial conditions, the dynamical evolution of a highly excited finite-size system creates a power law distribution of fragments with a critical exponent $\tau \approx 2.2$ [4]. This critical exponent has been found notably in the case of fragmentation of hydrogen cluster ions induced by a collision at 60 keV/u projectile energies [5] and in the case of fragmentation of nuclei induced by GeV proton impact [6]. These latter features, usually connected with multi-fragmentation processes, could be reminiscent of a second order phase transition in an infinite system [4]. Similar fragment mass distributions have been observed in the fragmentation of C_{60} induced by collisions [7,8]. Atomic collision techniques offer a powerful tool for investigation of the dynamics of highly excited finite-size systems. In our experiments, energy transfer can exceed that involved in previous work on cluster-atom collision by several orders of magnitude. The high values of the projectile velocity result in excitation processes differing significantly from those observed in studies performed with lower-energy beams or other excitation techniques. Here, we report on a direct observation of multi-ionization and multi-fragmentation of the H_{21}^+ cluster in a single collision with a helium atom at 60 keV/u using coincidence techniques.

2. Experimental

Our measurements were performed with H_{21}^+ cluster ions which can be regarded as a cluster of nine H_2 molecules around a H_3^+ core. The H_{21}^+ clusters at 1.26 MeV energy were delivered by the high-energy cluster-beam facility of the Institut de Physique Nucléaire de Lyon. The experimental apparatus has been described in detail in ref [9,10]. In brief, mass selected ionic H_{21}^+ clusters interact with helium atoms from a gas jet under single collision conditions. The

charged fragments resulting from the cluster fragmentation were deflected by a magnetic field 0.3μs after the interaction. Coincidence measurements were performed for the H_3^+ fragments [10] and the neutral fragments [11]. These fragments were detected with two surface barrier detectors. The peak amplitude of the signals given by the detectors was coded with a AD413A module (EG&G ORTEC) used in the coincidence mode. A master gate signal, derived from the signal given by the detector of neutral fragments, caused the two analog inputs to be grouped as a set of coincident events. Each set of coincident events was saved as a fragmentation event and can be sort using various conditions. The width of the master gate pulse was 2.5 μs and the intensity of the cluster beam was lowered to 1000 clusters/second to avoid fragmentation of two incident clusters during this time window.

3. Results and Discussion

A typical spectrum obtained with the H_3^+ fragment detector for the 60 keV/u - H_{21}^+ clusters colliding with a helium atom is displayed in Fig. 1. We observe three separate peaks at energies of 180, 360 and 540 keV, corresponding to the detection of one, two, and three H_3^+ originating from the same cluster [10]. From the growth rate method, the cross section for production of at least one H_3^+, σ_3, has been measured and found to be equal to $(14.0\pm1.4)10^{-16}$ cm^2.

The spectrum obtained with the neutral fragment detector is displayed in Fig. 2(a). It shows 20 separate peaks the energies of which range from 0.12 to 1.26 MeV. All neutral fragments coming from one incident cluster are detected simultaneously. Thus, in this spectrum, each event corresponds to a fragmentation of one incident cluster. The number ($S_{neutral}$) associated with each peak ($S_{neutral}$ = 2,3,4,...,21) corresponds to the value of the sum of the mass numbers of all the neutral fragments resulting from the fragmentation of one cluster. Later on, we will call a $S_{neutral}$ event a fragmentation event for which the sum of the mass numbers of all the neutral fragments is equal to $S_{neutral}$. As an example, $S_{neutral}$ = 10 is associated with the peak at the energy of 600 keV corresponding to the simultaneous detection of 10 mass units. Fragmentation events with $S_{neutral}$ = 0 and $S_{neutral}$ = 1 were not detected. The cross section for production of at least one neutral fragment, $\sigma_{neutral}$, has been measured and found to be equal to $(23.9\pm2.4)\ 10^{-16}$ cm^2. The H_{21}^+ cluster dissociation cross section measured in this experiment has been found to be equal to $(25.9\pm2.6)\ 10^{-16}$ cm^2, in good agreement with previous measurements [9]. Taking into account the

uncertainties, $\sigma_{neutral}$ is not significantly smaller than the dissociation cross section. Thus, most of the fragmentation events are detected. Among the events of the spectrum displayed in Fig. 2(a), we have selected those events which were in coincidence with the production of at least one H_3^+ fragment (59% of the total number of events). The spectrum of the events in coincidence with at least one H_3^+ fragment is displayed in Fig. 2(b). It shows 11 significant peaks at energies ranging from 0.48 to 1.08 MeV, associated with $S_{neutral}$ values from 8 to 18.

The spectra presented in Fig. 3 were obtained by selecting the events which were in coincidence with the production of one, two, and three H_3^+ fragments. The spectrum 3(a) corresponding to the events in coincidence with one H_3^+ fragment shows 11 peaks the energies of which range from 0.48 to 1.08 MeV. The spectrum 3(b) corresponding to the events in coincidence with two H_3^+ fragments shows 7 peaks with energies from 0.48 to 0.9 MeV. The spectrum 3(c) corresponding to the events in coincidence with three H_3^+ shows 5 peaks with energies from 0.48 to 0.72 MeV. As expected, the maximum value of $S_{neutral}$ observed decreased by three mass units with each incremental increase in the number of detected H_3^+ fragments. Note the varying heights of the particular peaks in the spectra. The shapes are very different from the hump shape observed in the spectrum of all the events (Fig. 2(a)).

In the spectra presented in Figures 1-3, spurious events (mainly due to collisions with the residual gas) have been subtracted as described in detail in ref. [10] and [11]. The spurious events correspond to about 1,7% of the incident cluster beam intensity in the case of the H_3^+ spectrum (Fig. 1), 5.5% in the case of the neutral spectrum (Fig. 2(a)), and 1,7% in the case of the coincident spectrum (Fig. 2(b)). The spectra in Figures 1-3, have been obtained for the same number of incident cluster ions and for a target thickness equal to $(0.95\pm0.09)\ 10^{14}$ atoms/cm^2. As an example, the coincidence spectra obtained without the helium gas target for the same number of incident cluster ions are presented in insets in Fig. 3. The target thickness used leads to a number of dissociated clusters equal to 20%, and thus, all the data are obtained under single-collision conditions [10].

From the branching ratio deduced from spectra (a) and (b) in Fig. 2, and from $\sigma_{neutral}$ and σ_3, we deduce the absolute production yield $\tau(S_{neutral})$ of $S_{neutral}$ events, and the absolute production yield $\tau_c(S_{neutral})$ of $S_{neutral}$ events in coincidence with at least one H_3^+ fragment, respectively. The

errors in the production yields deduced from these measurements vary from ±10% to ±15% taking into account uncertainty in the target thickness and statistical uncertainties. The histogram of $\tau(S_{neutral})$ versus $S_{neutral}$ is shown Fig. 4. The contribution of the events which are in coincidence with at least one H_3^+ fragment, $\tau_c(S_{neutral})$, is shown in dark grey. Fig. 4 shows also the contribution of the neutral events with no H_3^+ fragment production (unshaded bars), $\tau_{nc}(S_{neutral})$, equal to $(\tau(S_{neutral})- \tau_c(S_{neutral}))$. The histogram of $\tau(S_{neutral})$ can be roughly divided into three $S_{neutral}$ value ranges corresponding to H_2 molecule evaporation ($S_{neutral}$=2,4, and 6) with $\tau(S_{neutral})$, decreasing with increasing $S_{neutral}$, to ionization ($7 \leq S_{neutral} \leq 20$) with $\tau(S_{neutral})$ exhibiting a characteristic "hump shape", and to electron capture ($S_{neutral}$=21) [11].

The two contributions to the total yield $\tau(S_{neutral})$ can be compared. As expected, no H_3^+ fragment production is observed in the $S_{neutral}$ range ($2 \leq S_{neutral} \leq 6$, even) connected with H_2 evaporation. We observe that $\tau_c(S_{neutral})$ contributes mainly to that part of the histogram where $\tau(S_{neutral})$ exhibits the characteristic hump shape. For $S_{neutral}$ values from 15 to 18, most of the $S_{neutral}$ events result from coincidence with at least one H_3^+ fragment production (from 75% to 95%). This is also evident for $S_{neutral}$ equal to 13 and to 11. However, for even $S_{neutral}$ values (10,12,14) an important contribution of fragmentation events with no H_3^+ fragment production can be clearly observed (more than 50%). Moreover, $\tau_{nc}(S_{neutral})$ decreases with decreasing $S_{neutral}$. These events may be interpreted as fragmentation of an unstable doubly-charged cluster emitting a dimer H_2^+. This corresponds to channels :

$$(H_{21}^{++}) \Rightarrow H_p^+ + H_2^+ + \text{neutral fragments } (S_{neutral}) \text{ with } p=5, 7, .. \text{ odd and } S_{neutral} = 19 - p.$$

The absolute production yields $\tau_{c1}(S_{neutral})$, $\tau_{c2}(S_{neutral})$, and $\tau_{c3}(S_{neutral})$, of $S_{neutral}$ events corresponding to the fragmentation events with the production of one, two, and three H_3^+ fragments, respectively, are presented in Fig. 5. They were deduced from the branching ratios of the spectra (a), (b), (c) (Fig. 3) and from σ_3^{one}, σ_3^{two}, and σ_3^{three}. The latter cross sections were deduced from the branching ratios of the spectrum in Fig.1, and from σ_3.

The histogram of $\tau_{c1}(S_{neutral})$ versus $S_{neutral}$ is given in Fig. 5(a). The highest value of $\tau_{c1}(S_{neutral})$ was found for $S_{neutral}$ = 16. These events correspond mainly to the fragmentation channel

$$(H_{21}^{++}) \Rightarrow H_3^+ + H_2^+ + \text{neutral fragments } (S_{neutral} = 16)$$

which has to be related to the fragmentation channel (p=3) described above. The fragmentation channel leading to the production of two H^+(giving also $S_{neutral} = 16$) is less probable since it corresponds to a double ionization. Nevertheless, it has to be noted that the magnitude of $\tau_{c1}(16)$, $(2.3\pm0.3)\ 10^{-16}\ cm^2$, is of the same order as $\tau_{nc}(14)$, $(2.1\pm0.2)\ 10^{-16}\ cm^2$. From a comparison of the values of $\tau_{nc}(10)$, $\tau_{nc}(12)$, $\tau_{nc}(14)$ one would expect a larger value for $\tau_{c1}(16)$. An important point in this histogram is a relatively high value of $\tau_{c1}(13)$, $(1.6\pm0.2)\ 10^{-16}\ cm^2$, which is connected with a fragmentation process different from the one discussed above :

$$(H_{21}^{++}) \rightarrow H_p^+ + H_3^+ + \text{neutral fragments } (S_{neutral}) \text{ with } p=5 \text{ and } S_{neutral} = 13.$$

The unstable doubly - charged cluster decays by the fragmentation process, but at least one of the fragments results from a rearrangement in the cluster after ionization. The value of $\tau_{c1}(11)$ (with p=7 and $S_{neutral} = 11$) and $\tau_{c1}(9)$ (with p=9 and $S_{neutral} = 9$) can be interpreted in the same way. The value of $\tau_{c1}(S_{neutral})$ is observed to decrease whith decreasing $S_{neutral}$. Another interesting feature of this histogram is $\tau_c(18)$ which corresponds to the production of one H_3^+ fragment and several neutral fragments. Its value, $(1.3\pm0.2)\ 10^{-16}\ cm^2$, is relatively high in comparison with the decreasing values of $\tau(2)$ $(=(1.3\pm0.2)\ 10^{-16}\ cm^2)$, $\tau(4)$ $(=(0.7\pm0.1)\ 10^{-16}\ cm^2)$, and $\tau(6)$ $(=(0.4\pm0.06)10^{-16}\ cm^2)$ related to sequential evaporation of H_2. We surmise that this is due to the various energy transfer processes which can occur in the collision, and it shows that a large amount of energy can be deposited in the cluster without changing its initial charge.

The histogram of $\tau_{c2}(S_{neutral})$ versus $S_{neutral}$ is given in Fig. 5(b). The fragmentation channels associated with product yield $\tau_{c2}(15)$ cannot be assigned unambiguously. It may be assigned mainly to the fragmentation channel $(H_{21}^{2+}) \Rightarrow H_3^+ + H_3^+ + \text{neutral fragments}$. This fragmentation channel is evidently related to the fragmentation of an unstable doubly - charged cluster, with a rearrangement after ionization. The magnitude of $\tau_{c2}(15)$, $(2.8\pm0.3)\ 10^{-16}\ cm^2$, is greater than $\tau_{c1}(13)$ $(=(1.6\pm0.2)\ 10^{-16}\ cm^2)$, as expected. For other product yields, however, unambiguous assignment of fragmentation channels is possible. Events with $S_{neutral} = 14$ correspond to the following fragmentation channel $(H_{21}^{3+}) \Rightarrow H^+ + 2H_3^+ + \text{neutral fragments}$

resulting from a double ionization of the cluster ion. In the same way, the events with $S_{neutral} = 12$ result from a triple ionization of the cluster. Indeed, in this case, the sum of the mass numbers of the neutral fragments is 12, and two H_3^+ ions are detected. Therefore, three mass units of charged fragments are missing. This undetected mass (which cannot be a H_3^+ fragment) corresponds to at least two charged fragments, one H_2^+ and one H^+. The detection of four charged fragments can be explained by a triple ionization of the incident cluster ion.

The histogram of $\tau_{c3}(S_{neutral})$ versus $S_{neutral}$ is given in Fig. 5(c). All these events correspond to multi-fragmentation channels, since three H_3^+ fragments were detected. We note that the triple H_3^+ fragment production was observed with the production of other charged fragments (66% of the events in this spectrum). Among these events, some channels are completely determined such as $H_{21}^{4+} \Rightarrow 3H_3^+ + H^+ +$ neutral fragments ($S_{neutral} = 11$). This corresponds to fragmentation events after a triple ionization of the incident cluster ion. As discussed for $S_{neutral} = 11$ in the spectrum (b) in Fig. 5, the events with $S_{neutral} = 9$ show that a quadruple ionization of the incident cluster ion may occur in a collision. A minimum value of the cross section of quadruple ionization is given by $\tau_{c3}(9)$ (= $(4\pm0.6)\ 10^{-19}$ cm^2). This cross section may be expected to be higher, since the observed multi-fragmentation channel requires formation of two H_3^+ in the cluster after the quadruple ionization. These events correspond to a fraction of $1.5\ 10^{-4}$ of all the fragmentation events. Such ionization of the incident cluster may result from different excitation mechanisms. Double ionization of one molecule may be assumed , however, this does not seem to be sufficient.The main mechanism is probably an ionization of several molecules (up to 4) at various sites of the cluster. Therefore, a higher ionization rate may be expected, with the increase of the number of molecules H_2 in the cluster (9 in the H_{21}^+ cluster).

Acknowledgement

The authors wish to thank J. Martin, R. Filliol, J. P. Lopez, H. Mathez for their expert technical assistance.

References

[1] T. D. Mark, Int. J. Mass Spectrom. Ion Processes **79**, 1 (1987) and ref. therein.

[2] H. Gohlich, T. Lange, T. Bergmann, and T. P. Martin, Phys. Rev. Lett. **65**, 748 (1990) and ref. therein.

[3] D. H. E. Gross, A.R. DeAngelis, H. R. Jaqaman, Pan Jicai, and R. Heck, Phys. Rev. Lett. **68**, 146 (1992).

[4] V. Latora, M. Belkacem, and A. Bonasera, Phys. Rev. Lett. **73**, 1765 (1994)

[5] B. Farizon, M. Farizon, M. J. Gaillard, E. Gerlic, S. Ouaskit, Proceedings of the Conference of Polyatomic impact on solids and related phenomena, Saint Malo, June 1993, Nucl. Instr. and Meth. in Phys Res **B88**, 86 (1994).; S. Ouaskit et al., Int. J. Mass Spectrom. Ion Processes **139**, 141 (1994).

[6] X. Campi, Nucl. Phys. **A495**, 259c (1989).

[7] P. Hvelplund, L. H. Andersen, H. K. Haugen, J. Linhard, D. C. Lorents, R. Malhotra and R. Ruoff, Phys. Rev. Lett. **69**, 1915 (1992).

[8] T. Lebrun, H. G. Berry, S. Cheng, R. W. Dunford, H. Esbensen, D. S. Gemmel, E. P. Kanter, and W. Bauer, Phys. Rev. Lett. **72**, 3965 (1994).

[9] S. Ouaskit, B. Farizon, M. Farizon, M. J. Gaillard, and E. Gerlic, Phys. Rev. **A49**, 1484 (1994).

[10] B. Farizon et al., Z. Phys. **D33**, 53 (1995).

[11] B. Farizon et al., Int. J. Mass Spectrom. Ion Processes **144**, 79 (1995).

Figure captions

Figure 1 : Fragmentation of 60 keV/u - H_{21}^+ clusters induced by a single collision with a helium atom. Spectrum obtained with the H_3^+ fragment detector.

Figure 2 : Fragmentation of 60 keV/u - H_{21}^+ clusters induced by a single collision with a helium atom. (a) Total spectrum obtained with the detector of neutral fragments. (b) Events in coincidence with the production of at least one H_3^+ fragment.

Figure 3 : Fragmentation of 60 keV/u - H_{21}^+ clusters induced by a single collision with a helium atom. Events are shown, which are in coincidence with the production of (a) one, (b) two and (c) three H_3^+ fragments. Inset : the same spectra but obtained without helium gas target for the same number of incident clusters.

Figure 4 : Fragmentation event production yields, $\tau(S_{neutral})$, versus $S_{neutral}$. The contribution of the events with at least one H_3^+ fragment production, $\tau_c(S_{neutral})$, is drawn in dark grey.

Figure 5 : Production yields, $\tau_{c1}(S_{neutral})$, $\tau_{c2}(S_{neutral})$, and $\tau_{c3}(S_{neutral})$, of fragmentation events with production of (a) one, (b) two, and (c) three H_3^+ fragments, versus $S_{neutral}$.

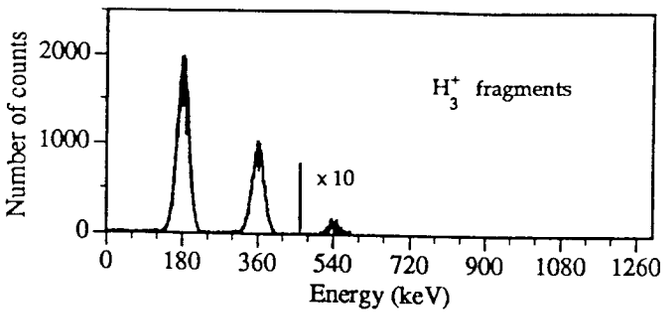

Figure 1

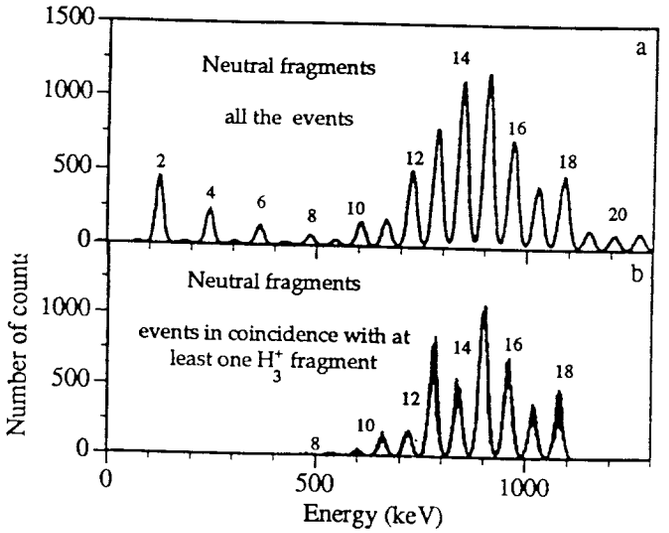

Figure 2

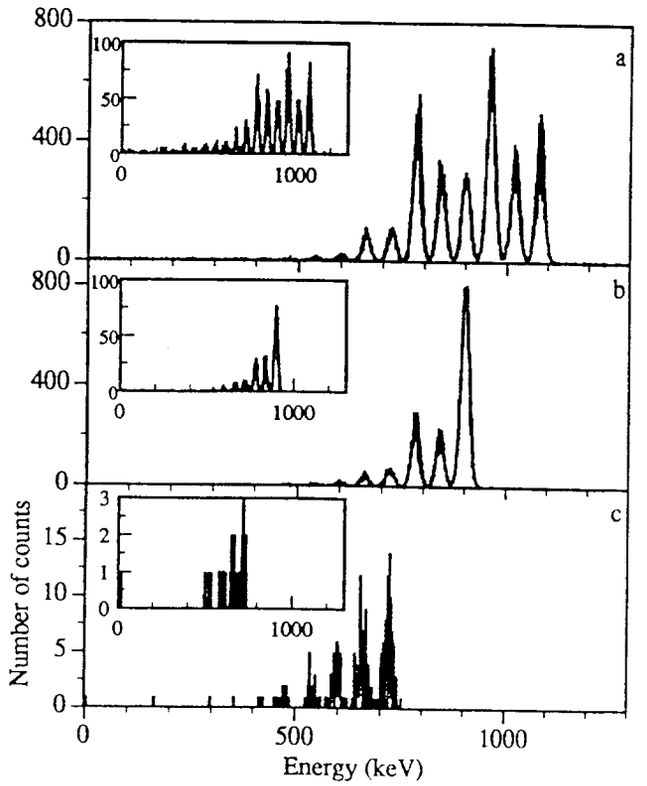

Figure 3

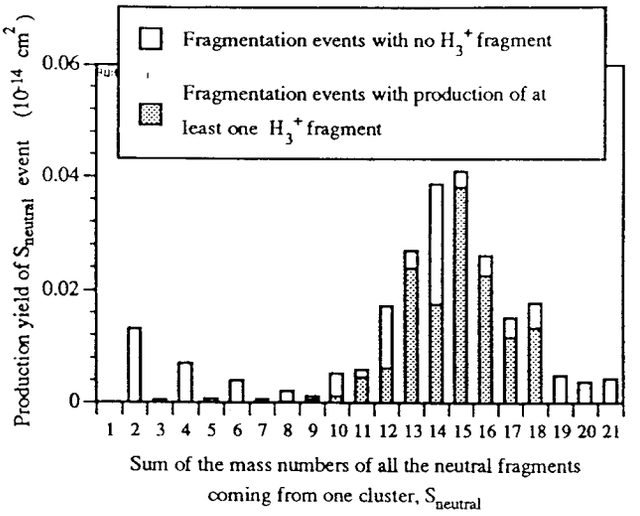

Figure 4

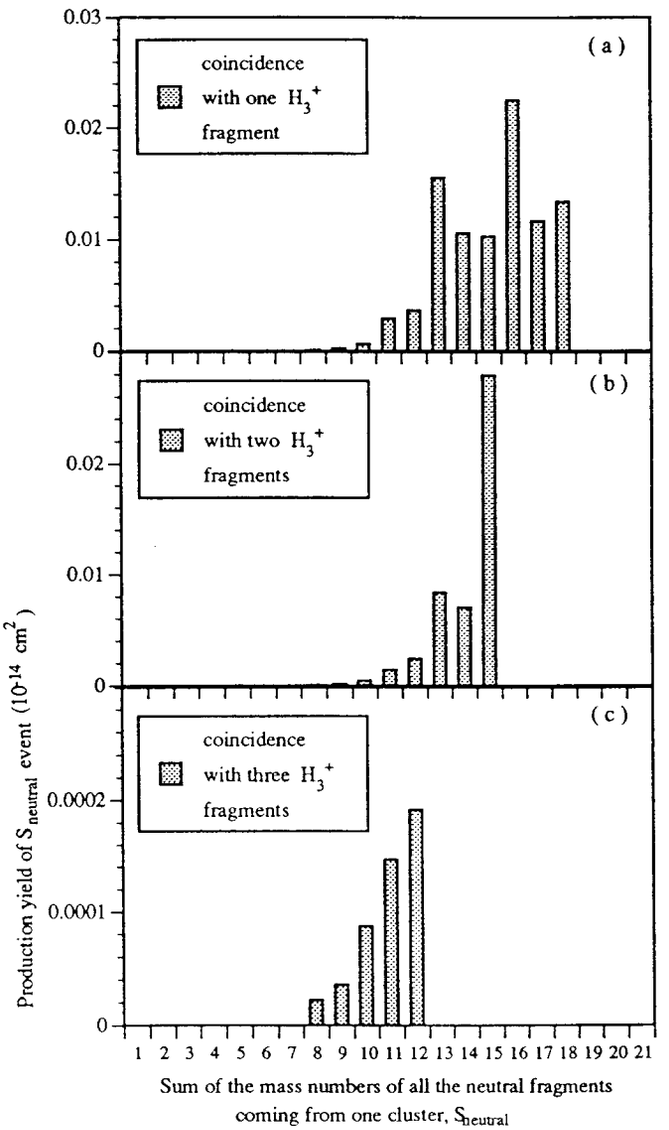

Figure 5